Available online at www.sciencedirect.com
ScienceDirect
Ceramics International 37 (2011) 21–27
CERAMICS INTERNATIONAL
www.elsevier.com/locate/ceramint

Isothermal sintering of barium–zinc–titanate ceramics

N. Obradović [a,*], S. Filipović [a], V. Pavlović [b], M. Mitrić [c], S. Marković [a], V. Mitić [a,d], N. Đorđević [e], M.M. Ristić [f]

[a] Institute of Technical Sciences SASA, Knez Mihailova 35/IV, 11000 Belgrade, Serbia
[b] Faculty of Agriculture, University of Belgrade, 11000 Belgrade, Serbia
[c] Vinca Institute, 11000 Belgrade, Serbia
[d] Faculty for Electronics, University of Niš, 18000 Niš, Serbia
[e] Institute for Technology of Nuclear and Other Row Materials, F. d'Eperey 86, 11000 Belgrade, Serbia
[f] Serbian Academy of Sciences and Arts, Knez Mihailova 35, 11000 Belgrade, Serbia

Received 10 March 2010; received in revised form 8 April 2010; accepted 14 June 2010
Available online 13 July 2010

Abstract

Mixtures of $BaCO_3$–ZnO–TiO_2 were mechanically activated using high-energy planetary ball mill during 20, 40 and 80 min. As the time of mechanical activation increased, the decrease in particle size was observed. The effect of milling on microstructure was investigated by scanning electron microscopy, as well. Sintering process was performed in air at 1100 and 1200 °C for 2 h. Various phases are present within mixtures sintered at 1100 and 1200 °C, and almost pure $BaZn_2Ti_4O_{11}$ phase was obtained after 80 min of milling and sintering at 1200 °C for 2 h.

Keywords: A. Milling; A. Sintering; B. X-ray methods; D. Traditional ceramics

1. Introduction

BaO–TiO_2 based materials with different Ba/Ti ratios have been investigated in the past years and have attracted great attention for their specific microwave properties. They are widely used in the MW region as the parts of resonators, filters and Multilayer Ceramic Capacitors [1]. Owing to their variety of applications, there has been a lot of interest in studying both their structure and properties [2]. In order to improve microwave properties of these materials, numerous additives, such as ZnO, MnO, SnO, etc. have been used [3–7]. Roth et al. [8] suggested the phase diagram of the ternary system BaO–ZnO–TiO_2 and reported the chemical composition of the compound $BaZn_2Ti_4O_{11}$, with the ratio of the starting oxides being close to 1:2:4.

In order to obtain the various barium–zinc–titanate phases, to lower the sintering temperature and/or to improve microwave properties, many synthesis routes, such as chemical processing, mechanical activation and additives usage, can be used [3–7]. Those methods typically produce large, non-uniform and agglomerated particles, which generally limits the ability to fabricate reliable electronic components [9]. One opportunity to influence initial powder microstructure and sintering properties of the material is to mechanically activate the powder using a high-energy milling process. These processes are a common way for producing fine nano materials and have many advantages; a low-cost, simple and ''applicable to any class of materials'' techniques. Unfortunately, no systematic investigations of mechanical activation influence on synthesis and sintering of BaO–ZnO–TiO_2 system have been performed. Furthermore, there is a lack of information on system itself since only few researchers [2,8] have been dealing with the $BaZn_2Ti_4O_{11}$ phase. Taking all this into account, in this article, the influence of mechanical activation on the structure, as well as the isothermal sintering of $BaCO_3$–ZnO–TiO_2 system, was studied. As a result, the authors revealed the relatively cheap, simple way, for obtaining the densed pure material with advantageous microstructures and phase composition.

2. Experimental procedure

Mixtures of $BaCO_3$ (99% Sigma–Aldrich), ZnO (99% Sigma–Aldrich) and TiO_2 powders (99.8% Sigma–Aldrich) at

* Corresponding author. Tel.: +381 11 20 27 203; fax: +381 11 2185 263.
E-mail address: obradovic.nina@yahoo.com (N. Obradović).

0272-8842/$36.00
doi:10.1016/j.ceramint.2010.07.001

a molar ratio $BaCO_3$:ZnO:TiO_2 = 1:2:4 were mechanically activated by grinding in a high-energy planetary ball mill device (Retsch type PH 100). The milling process was performed in air for 20, 40 and 80 min at a basic disc rotation speed of 400 rpm. Zirconium oxide balls (approx. 10 mm in diameter) and bowls (250 cm^3) were used with a ball to powder mixture mass ratio of 20:1. Samples were denoted as BZT-0 to BZT-80, according to the milling time.

The morphology of obtained powders and sintered mixtures was characterized by scanning electron microscopy (JEOL JSM-6390 LV). The powders were crushed and covered with gold in order to perform these measurements.

The average particle size, particle size distribution, and the nature of agglomerates were determined by particle size analyzer (PSA). The used instrument was Mastersizer 2000 (Malvern Instruments Ltd., UK) particle size analyzer based on laser diffraction, which covers the particle size range of 0.02–2000 μm. For the PSA measurements, the powders were dispersed in distilled water, in ultrasonic bath (low-intensity ultrasound, at a frequency of 40 kHz and power of 50 W), for 5 min.

X-ray powder diffraction patterns after milling and sintering were obtained using a Philips PW-1050 diffractometer with λCu Kα radiation and a step/time scan mode of 0.05°/1 s.

The binder-free powders were compacted using the uniaxial double action pressing process in an 8 mm diameter tool (Hydraulic press RING, P-14, VEB THURINGER). Compacts were placed in an alumna boat and heated in a tube furnace (Lenton Thermal Design Typ 1600). Compacts were sintered isothermally at 1100 and 1200 °C in air atmosphere for 120 min, the heating rate was 10 °C/min. The density of specimens was calculated from precise measurements of specimen's diameter, thickness and mass.

3. Results and discussion

It is well known that during mechanical attrition by ball milling, the evolution of material phases is coupled to the mechanical properties of the powders and therefore to their microstructures [10]. It has been established that the microstructure evolution is controlled by the temperature, milling intensity and composition. The grain size, internal lattice strain and stored enthalpy are parameters characterized by most authors [11]. Our microstructure analyses of $BaCO_3$–ZnO–TiO_2 system showed that the initial $BaCO_3$ powder consisted of irregularly shaped agglomerates with a size of 2 μm approximately. Compared to $BaCO_3$ particles, ZnO and TiO_2 spherical particles were smaller with the particles with a size of 200 nm. It has been observed that the grain size of the starting powder mixture, decreased with milling time, approaching a steady state after prolonged milling time. BZT-0 micrograph presented in Fig. 1(a) indicated that the $BaCO_3$ particles probably served as nuclei and have been layered over by ZnO and TiO_2 particles.

As a result of particles having deformation introduced by mechanical activation, the formation of soft agglomerates and new needle shaped grains, has been noticed in SEM micrographs of BZT-20. Micrographs of BZT-40 and BZT-80 clearly indicated the presence of several phases within hard agglomerates covered with smaller particles of starting powders (Fig. 1(c) and (d)).

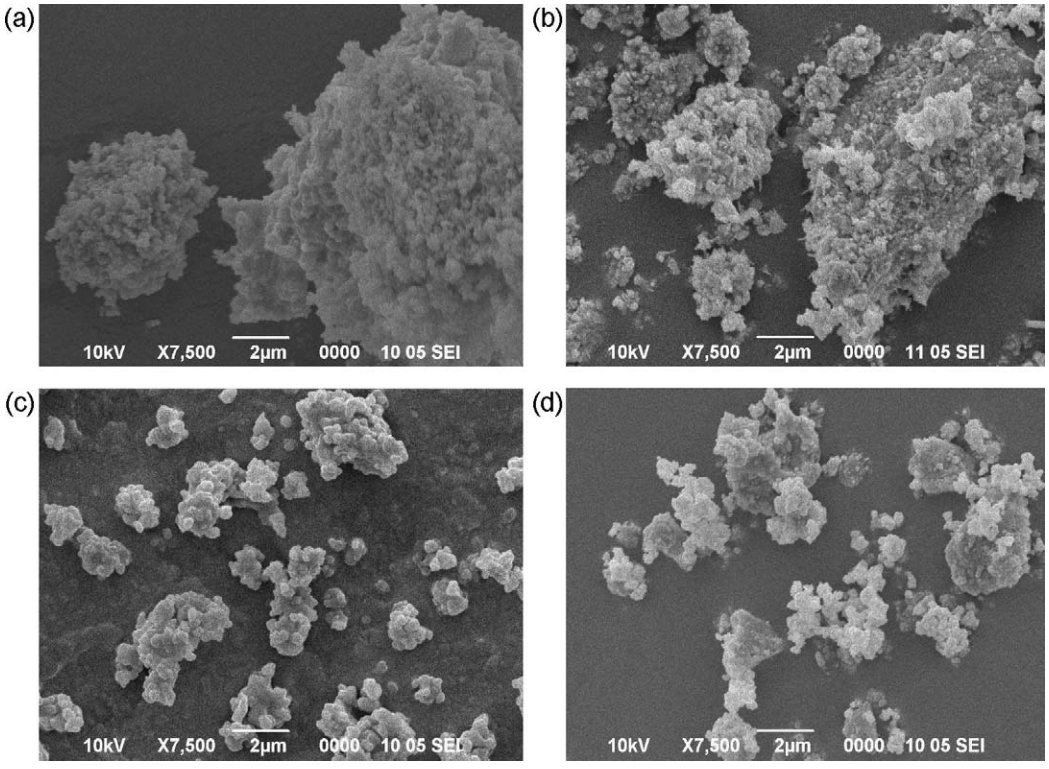

Fig. 1. Scanning electron micrographs of (a) BZT-0, (b) BZT-20, (c) BZT-40 and (d) BZT-80.

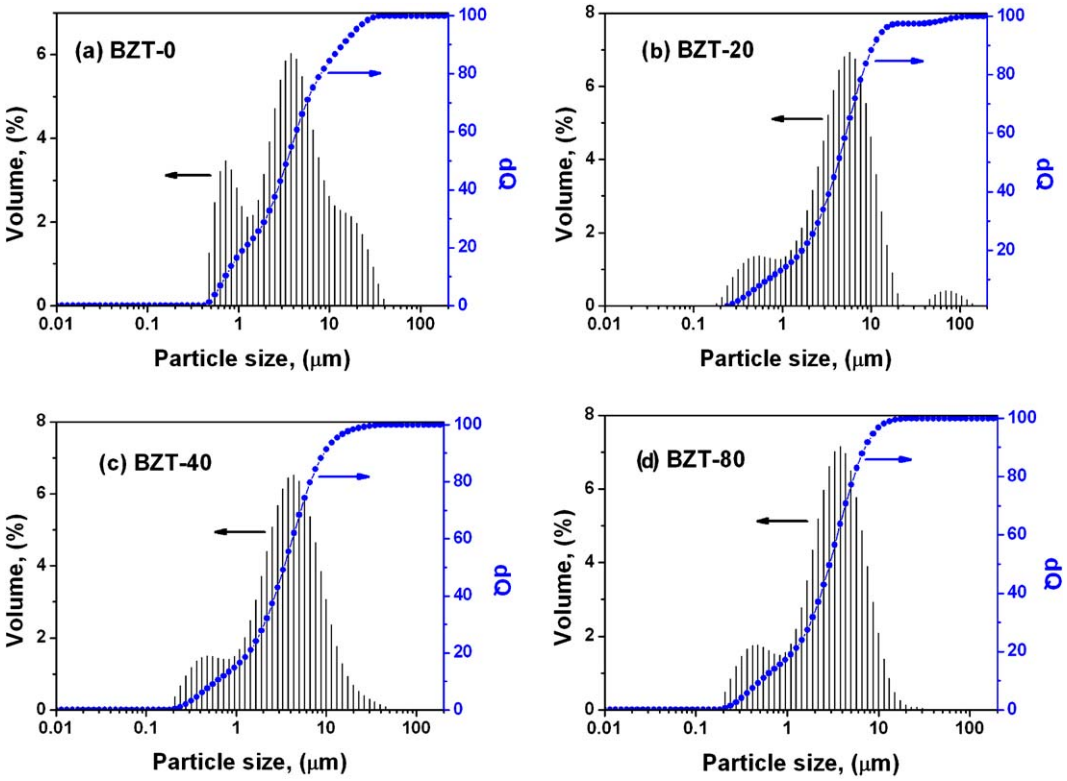

Fig. 2. Cumulative and frequency distribution curves for (a) BZT-0, (b) BZT-20, (c) BZT-40 and (d) BZT-80.

Fig. 2 shows frequency distribution and cumulative distribution curves of all samples. Fig. 2(a) shows that the BZT-0 particle size distribution is consisted of two differently sized particles. The first one were about 0.7 μm, and the second one contained particles that are about 3.5 μm in size and a "shoulder" representing a small part of bigger particles approximately 20 μm in size. Particle size distribution of the starting powder mixture represents small particles of TiO_2, bigger particles of ZnO and $BaCO_3$ agglomerates, respectively, which is in accordance with BZT-0 micrograph. Fig. 2(b) shows a third kind of particles, with distribution at around 65 μm, indicating that some new phases have been formed, in shape of soft agglomerates that were easily broken with prolonged milling time.

Furthermore, we suppose that the BZT-40 and BZT-80 particle size distributions belong to the two differently sized agglomerates – about 0.4, and 4 μm within BZT-40 and 0.4 and, finally, 3.5 μm within BZT-80, representing the agglomerates of some new phases, covered with smaller ones of starting powders, which is in a great accordance with the given micrographs.

This is in accordance with the X-ray analysis, which pointed out that mechanical activation of $BaCO_3$–ZnO–TiO_2 system is not only characterized by crystallite size reduction and increase in dislocation density and lattice strain [12], but also by formation of new barium–titanate and zinc–titanate phases.

X-ray diffraction patterns of non-milled and ball-milled $BaCO_3$, ZnO and TiO_2 powders are given in Fig. 3. BZT-0 is the X-ray pattern of the non-milled starting mixture containing $BaCO_3$, ZnO and TiO_2 (anatase and rutile modification). The identification of all obtained reflections has been accomplished using the JCPDS cards (86-1157 for TiO_2 anatase, 71-2394 for $BaCO_3$, 89-0510 for ZnO, 76-0326 for TiO_2 rutile, 75-1582 TiO_2 brookite, 87-1781 for $Zn_2Ti_3O_8$, 82-1175 for $BaTiO_3$ and 85-0547 for $ZnTiO_3$). After 5 min of mechanical treatment, intensities of all peaks are lowered. Also, the third modification of TiO_2, brookite, is observed within mixture activated for 5 min along with the very first traces of metastable compound $Zn_2Ti_3O_8$.

The peak's lowering is continued within BZT-10 diffraction pattern. Also, the very first traces of a new $BaTiO_3$ phase are observed. BZT-20 diffraction pattern indicated that the process of amorphization is taking place along with peak broadening. We can also notice the appearance of $ZnTiO_3$ phase and disappearance of TiO_2 rutile and brookite phases.

The decrease of crystallinity that takes place in this type of powder processing is a consequence of defect formation and diminuition of crystallite size causing peak broadening. Moreover, as the time of activation is prolonged, the less intensities and greater broadening of all peaks are observed. In the BZT-40 pattern, we can notice the simultaneous decrease of TiO_2 anatase, ZnO and $BaCO_3$ with an increase of $BaTiO_3$, $ZnTiO_3$ and $Zn_2Ti_3O_8$ phases. After 80 min of activation, all phases mentioned above within BZT-40 are still present, although the dominant phase is a phase of $BaTiO_3$.

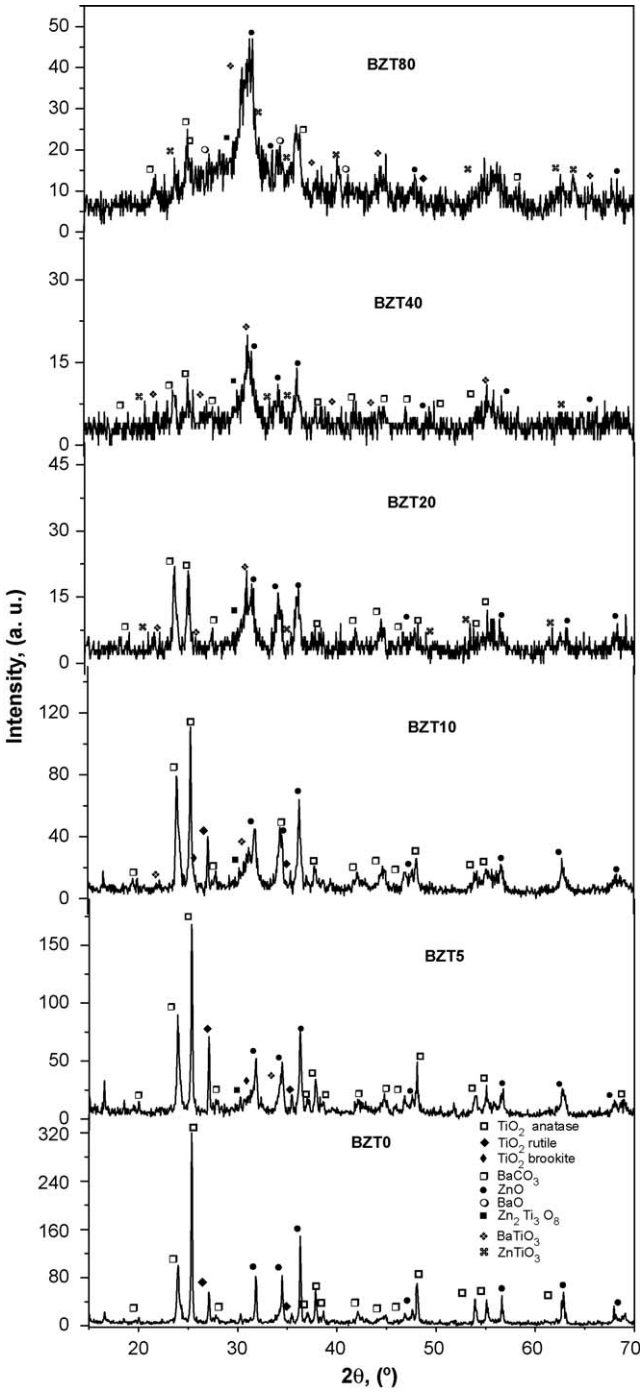

Fig. 3. XRD patterns of non-milled and ball-milled powder mixtures.

Microstructure parameters revealed from an approximation method [13] of ball-milled powder mixtures: average particle size (D), density of dislocations (ρ_D) and lattice strain (e_{hkl}) are given in Table 1. Tribophysical activation is characterized by crystallite size reduction and increase of dislocation density and lattice strain [14–16], and our experiment confirmed these facts. Tribophysical activation leads to the reduction in cohesive dispersion domains for all directions observed, the number of defects within the material rises and that reclaims the diffusion of ZnO, $BaCO_3$ and TiO_2 atoms, which leads to a solid-state reaction. These calculations have been conducted for the most intensive reflections of ZnO (1 0 0), (0 0 2) and (1 0 1), TiO_2–anatase (1 0 1) and (2 0 0) and $BaCO_3$ (1 1 1). As the time of activation increased, some of the calculations were not possible to conduct due to great peak broadening and overlapping with some reflections of the final products. Analyses of microstructure parameters calculated from the XRD data indicate that the most intense changes are present in the ZnO lattice and it is obvious that the crystallite size of ZnO decreases most during the milling process, for all three directions observed here. We can say that the process of ZnO crystal lattice destruction is the dominant one owing to greater hardness of TiO_2 and $BaCO_3$.

Fig. 4 represents densities obtained after the compaction process and after the sintering process at 1100 and 1200 °C for 2 h. The maximum change in densification rate is observed within powders activated 20 min. It is also clearly visible that the greater densities are obtained after 40 and 80 min of activation, but not the expected ones, they are very similar to the ones obtained after 20 min.

Some of our previous investigations [17–19] are indicating at the same problem about densification during the sintering process. Namely, after certain time of milling (15 or 20 min, depending on the balls to powder mass ratio), curves got into the saturation part and further activation does not influence the density increase. Regarding previous analysis based on SEM micrographs, it is clear why prolonged mechanical activation inhibits densification. Namely, it is known that a high content of hard agglomerates, that are present within BZT-40 and BZT-80 in a higher content than in ones activated 20 min, is not suitable for good sinterability.

Samples activated and sintered at 1100 °C for 2 h, presented in Fig. 5, do not posses the same structure as the non-activated sintered ones. XRD patterns of non-activated sintered samples indicated that several phases: $BaTiO_3$, $ZnTiO_3$, $Ba_4ZnTi_{11}O_{27}$ and $BaZn_2Ti_4O_{11}$ are present within a mixture BZT-0 sintered at 1100 °C for 2 h. In activated and sintered samples, the absence of $BaTiO_3$ and $Ba_4ZnTi_{11}O_{27}$ was noticed, along with the decrease in $ZnTiO_3$ concentration.

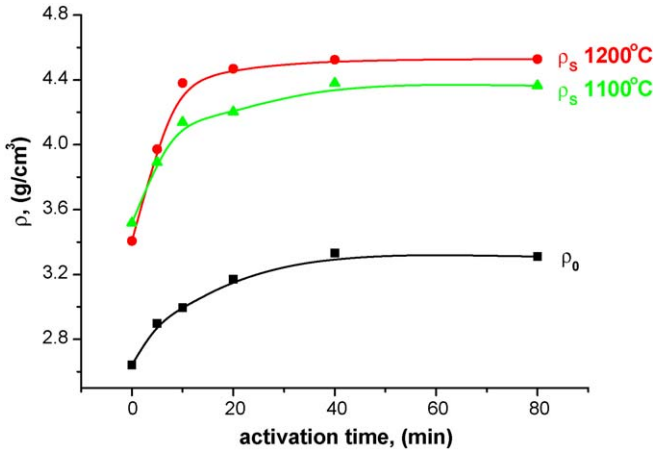

Fig. 4. Densities of compacts before sintering and after isothermal sintering for 2 h.

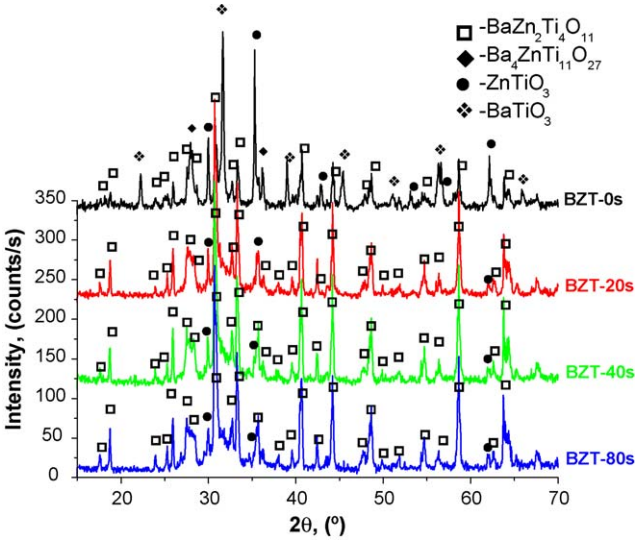

Fig. 5. XRD patterns of mixtures sintered at 1100 °C for 2 h.

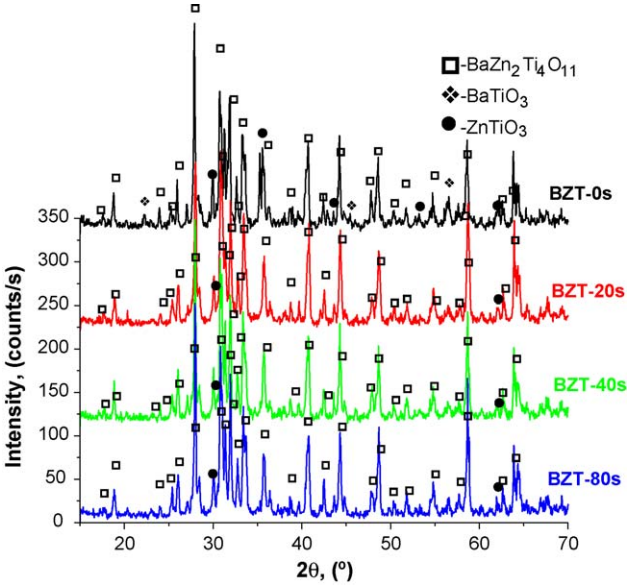

Fig. 6. XRD patterns of mixtures sintered at 1200 °C for 2 h.

No pure phase has been obtained within mixtures sintered at 1200 °C although the $Ba_4ZnTi_{11}O_{27}$ phase is not present. Based on the analysis of peak's intensities, the concentration of $ZnTiO_3$ phase is decreasing with the increase in milling time. Furthermore, no $BaTiO_3$ phase is observed within activated and sintered samples. The almost pure $BaZn_2Ti_4O_{11}$ phase along with a very small concentration of $ZnTiO_3$ phase is obtained after 80 min of milling and sintering at 1200 °C for 2 h, presented in Fig. 6.

Micrographs of the samples sintered at 1200 °C for 2 h are given in Fig. 7. TiO_2 has not reacted completely, forming the liquid phase. Breakage throughout grains of very soft zinc–titanate phase along with large porosity are the main characteristics of non-activated sintered sample. Fig. 7(b) indicated at grains smaller than 1 μm, larger grains of 2 μm in size and the third type are grains 10 μm in size along with open porosity and ZnO in accession. Formation of spheroidal and closed pores as a consequence of barium–zinc–titanate blocks

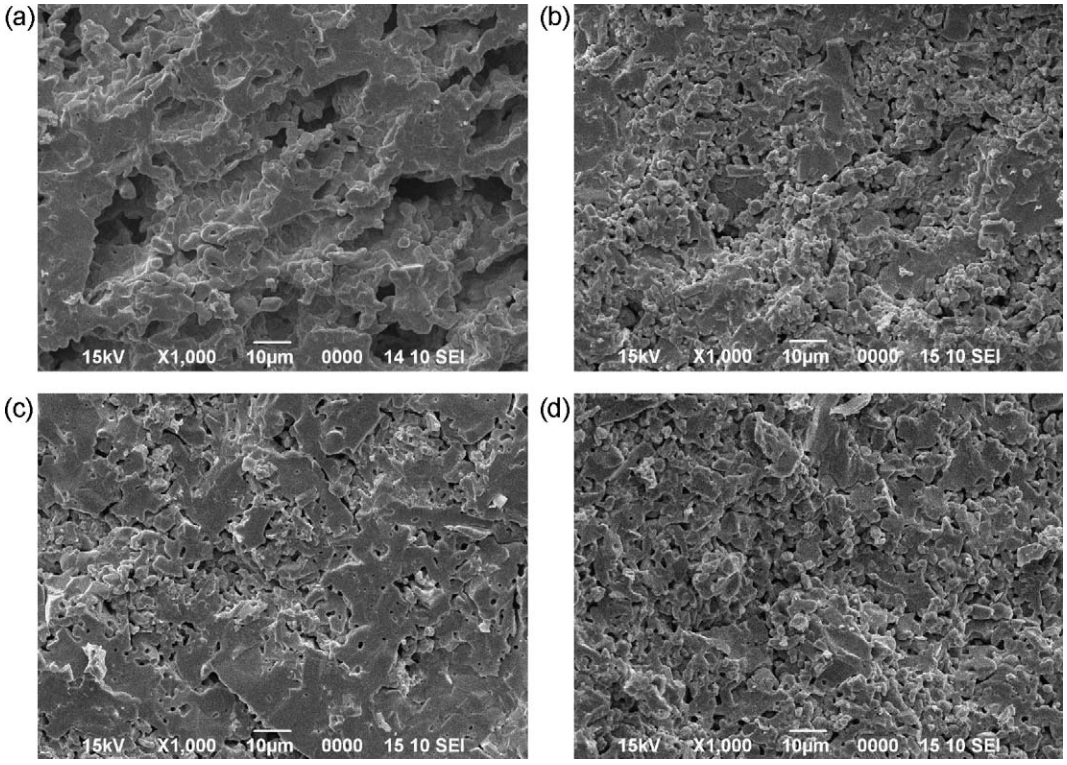

Fig. 7. Scanning electron micrographs of (a) BZT-0, (b) BZT-20, (c) BZT-40 and (d) BZT-80 sintered at 1200 °C for 2 h.

Table 1
Microstructure parameters revealed from an approximation method.

Sample	Phase	D (nm)						ρ_D ($\times 10^{10}$ cm^{-2})						e_{hkl} 10					
		1 0 0	0 0 2	1 0 1	1 0 1	2 0 0	1 1 1	1 0 0	0 0 2	1 0 1	1 0 1	2 0 0	1 1 1	1 0 0	0 0 2	1 0 1	1 0 1	2 0 0	1 1 1
	ZnO	72	73	112				6	6	2				1.7	1.6	0.9			
BZT-0	TiO_2				80	64					5	7					1.9	1.3	
	$BaCO_3$						52						11						3.2
	ZnO	47	32	56				14	29	9				2.7	3.7	1.9			
BZT-5	TiO_2				70	58					6	9					2.3	1.5	
	$BaCO_3$						46						14						3.6
	ZnO	23	23	36				57	57	23				5.5	5.0	3.1			
BZT-10	TiO_2				57	35					9	24					2.8	2.4	
	$BaCO_3$						35						24						4.8
	ZnO	–	23	31				–	57	31				–	5.0	3.5			
BZT-20	TiO_2				35	–					23	–					4.5	–	
	$BaCO_3$						31						31						5.4

approaching each other increased the density and are determining the sample activated 40 min and sintered. Furthermore, well formed barium–zinc–titanate phase with no visible traces of ZnO is observed within sintered BZT-80 mixture. One can notice that samples activated 80 min and sintered have advantageous microstructures, with the appropriate pores/materials ratio.

4. Conclusion

In this paper, the influence of mechanical activation on the structure, as well as the isothermal sintering of $BaCO_3$–ZnO–TiO_2 system, was studied. Scanning electron micrographs indicated a difference between the starting and activated powders morphology, confirming the changes taking place during the mechanical activation. Having in mind results based on PSA measurements, it has been found, that frequency distribution and cumulative distribution curves, indicated at particle size reduction during mechanical treatment up to 20 min, along with the formation of new phases and after that time agglomeration process has been noticed.

XRD data gave information on phase composition of sintered samples. 1100 °C is the temperature where one can notice the existence of several phases, such as $BaTiO_3$, $ZnTiO_3$, $Ba_4ZnTi_{11}O_{27}$ and $BaZn_2Ti_4O_{11}$. With the prolonged milling time and increasing sintering temperature, the disappearance of $BaTiO_3$ and $Ba_4ZnTi_{11}O_{27}$ phases and the decrease in $ZnTiO_3$ phase concentration along with the increase in $BaZn_2Ti_4O_{11}$ has been observed. 80 min of activation and sintering at 1200 °C for 2 h are the used conditions where the almost pure $BaZn_2Ti_4O_{11}$ phase has been obtained, with density that is above 92% of TD of barium–zinc–titanate.

Acknowledgements

This research was performed within the projects 142011 G, financed by the Ministry for Science of the Republic of Serbia and project F-7/II financed by Serbian Academy of Sciences and Arts.

References

[1] W. Guoquing, W. Shunhua, S. Hao, Microwave dielectric ceramics in the BaO–TiO_2–ZnO system doped with $MnCO_3$ and SnO_2, Mater. Lett. 59 (2005) 2229–2231.
[2] A. Belous, O. Ovchar, M. Macek-Krzmanc, M. Valant, The homogeneity range and microwave dielectric properties of the $BaZn_2Ti_4O_{11}$ ceramics, J. Eur. Ceram. Soc. 26 (2006) 3733–3739.
[3] J.-H. Choy, Y.-S. Han, S.-H. Hwang, Citrate route to Sn-doped $BaTi_4O_9$ with microwave dielectric properties, J. Am. Ceram. Soc. 81 (1998) 3197–3204.
[4] K.H. Yoon, J.B. Kim, W.S. Kim, E.S. Kim, Effect of $BaSnO_3$ on the microwave dielectric properties of $BaTi_9O_{20}$, J. Mater. Res. 11 (1996) 1996–2001.
[5] T. Negas, G. Yeager, S. Bell, N. Coats, $BaTi_4O_9$/$Ba_2Ti_9O_{20}$-based ceramics resurrected for modern microwave applications, Am. Ceram. Soc. Bull. 72 (1993) 80–89.
[6] X. Wang, M. Gu, B. Yang, S. Zhu, W. CaO, Hall effect and dielectric properties of Mn-doped barium titanate, Microelectron. Eng. 66 (2003) 855–859.
[7] W.-Y. Lin, R.F. Speyer, W.S. Hackenberger, T.R. Shrout, Microwave properties of $Ba_2Ti_9O_{20}$ doped with zirconium and tin oxides, J. Am. Ceram. Soc. 82 (1999) 1207–1211.
[8] R.S. Roth, C.J. Rawn, C.G. Lindsay, W. Wong-Ng, Phase equilibria and crystal chemistry of the binary and ternary barium polytitanates and crystallography of barium zinc polytitanates, J. Solid State Chem. 104 (1993) 99–118.
[9] V.P. Pavlović, M.V. Nikolić, Z. Nikolić, G. Branković, Lj. Živković, V.B. Pavlović, M.M. Ristić, Microstructural evolution and electric properties of mechanically activated $BaTiO_3$ ceramics, J. Eur. Ceram. Soc. 27 (2007) 575–579.
[10] J. Xu, G.S. Collins, L. Peng, M. Atzmon, Deformation-assisted decomposition of unstable $Fe_{50}Cu_{50}$ solid solution during low-energy ball milling, Acta Mater. 47 (1999) 1241–1245.
[11] H.H. Tiam, M. Atzmon, Kinetics of microstructure evolution in nanocrystalline Fe powder during mechanical attrition, Acta Mater. 47 (1999) 1255–1259.
[12] N. Obradović, N. Labus, T. Srećković, D. Minić, M.M. Ristić, Synthesis and characterization of zinc titanate nano-crystal powders obtained by mechanical activation, Sci. Sint. 37 (2005) 123–129.
[13] Lj. Karanović, Applied Crystallography, Belgrade University, Belgrade, 1996, p. 91 (in Serbian).
[14] M.G. Kakazey, L.A. Klockov, I.I. Timofeeva, T.V. Srećković, B.A. Marinković, M.M. Ristić, Evolution of the defect structure of zinc-oxide as a consequence of tribophysical activation, Cryst. Res. Technol. 34 (1999) 859–866.
[15] M.G. Kakazey, V.A. Melnikova, T.V. Srećković, T.V. Tomila, M.M. Ristić, Evolution of the microstructure of disperse zinc-oxide during tribophysical activation, J. Mater. Sci. 34 (1999) 1691–1697.

[16] N. Obradović, N. Labus, T. Srećković, M.M. Ristić, The influence of tribophysical activation on Zn_2TiO_4 synthesis, Mater. Sci. Forum 518 (2006) 131–136.
[17] T. Srećković, N. Labus, N. Obradović, Lj. Živković, Enchancing synthesis and sintering of zinc titanate using mechanical activation, Mater. Sci. Forum 453 (2004) 435–440.
[18] N. Obradović, N. Labus, T. Srećković, S. Stevanović, Reaction sintering of $2ZnO–TiO_2$ system, Sci. Sint. 39 (2007) 127–132.
[19] N. Obradović, S. Stevanović, M. Mitrić, M.V. Nikolić, M.M. Ristić, Analysis of isothermal sintering of zinc titanate doped with MgO, Sci. Sint. 39 (2007) 241–248.